Mission Analysis and Aircraft Sizing of a Hybrid-Electric Regional Aircraft

Kevin R. Antcliff[1], Mark D. Guynn[2], Ty V. Marien[3], and Douglas P. Wells[4]
NASA Langley Research Center, Hampton, VA, 23681

Steven J. Schneider[5] and Michael T. Tong[6]
NASA Glenn Research Center, Cleveland, OH 44135

The purpose of this study was to explore advanced airframe and propulsion technologies for a small regional transport aircraft concept (~50 passengers), with the goal of creating a conceptual design that delivers significant cost and performance advantages over current aircraft in that class. In turn, this could encourage airlines to open up new markets, reestablish service at smaller airports, and increase mobility and connectivity for all passengers. To meet these study goals, hybrid-electric propulsion was analyzed as the primary enabling technology. The advanced regional aircraft is analyzed with four levels of electrification, 0% electric with 100% conventional, 25% electric with 75% conventional, 50% electric with 50% conventional, and 75% electric with 25% conventional for comparison purposes. Engine models were developed to represent projected future turboprop engine performance with advanced technology and estimates of the engine weights and flowpath dimensions were developed. A low-order multi-disciplinary optimization (MDO) environment was created that could capture the unique features of parallel hybrid-electric aircraft. It is determined that at the size and range of the advanced turboprop: The battery specific energy must be 750 Wh/kg or greater for the total energy to be less than for a conventional aircraft. A hybrid vehicle would likely not be economically feasible with a battery specific energy of 500 or 750 Wh/kg based on the higher gross weight, operating empty weight, and energy costs compared to a conventional turboprop. The battery specific energy would need to reach 1000 Wh/kg by 2030 to make the electrification of its propulsion an economically feasible option. A shorter range and/or an altered propulsion-airframe integration could provide more favorable results.

I. Introduction

THE prospect of electric motors and electric power being used for aircraft propulsion has been an appealing notion for some time. Recently, this idea has morphed into a compelling business case due to significant technological advancements in electric motors and batteries. There are currently no mass-produced hybrid-electric or all-electric aircraft available. However, with the introduction of the Airbus E-Fan and other similar concepts, it will not be long before such vehicles are produced.[1]

The purpose of this study was to explore advanced airframe and propulsion technologies for a small regional transport aircraft concept (~50 passengers), with the goal of creating a conceptual design that delivers significant cost and performance advantages over current aircraft in that class. The first part of this study focused on defining the requirements, assessing promising airframe and propulsion technologies, and selecting a vehicle concept. As the primary enabling technology, hybrid-electric propulsion was chosen to meet the study objectives of increasing safety, affordability, environmental compatibility, and customer acceptance. There are currently a number of NASA activities related to hybrid-electric aircraft propulsion that could enable such a propulsion system in the future. The second part of the study focused on determining the sizing and performance of the hybrid-electric aircraft concept. The subject of

[1] Aerospace Engineer, Aeronautics Systems Analysis Branch, MS 442, Member AIAA.
[2] Aerospace Engineer, Aeronautics Systems Analysis Branch, MS 442, Senior Member AIAA.
[3] Aerospace Engineer, Aeronautics Systems Analysis Branch, MS 442.
[4] Aerospace Engineer, Aeronautics Systems Analysis Branch, MS 442, Senior Member AIAA.
[5] Aerospace Engineer, Chemical and Thermal Propulsion Systems Branch, MS 5-11, Associate Fellow AIAA.
[6] Aerospace Engineer, Propulsion Systems Analysis Branch, MS 5-11.

this paper is the sizing and mission analysis effort, and the associated tool development. A regional transport aircraft concept employing hybrid-electric propulsion is analyzed and compared to an advanced aircraft with conventional propulsion. The parallel hybrid-electric propulsion architecture presented in this study consists of a turbine engine driving a propeller, with additional power provided by an electric motor attached to the turbine shaft. A separate power source (e.g. battery) provides electrical power to the motor. A methodology is presented for the sizing and mission performance analysis of the parallel architecture hybrid-electric regional aircraft. Multiple trade studies are presented that examine the effect of battery specific energy (BSE) and propulsion electrification (the power provided by the battery as opposed to the power provided by the turbine) on aircraft sizing, performance, and energy cost.

II. Background

In the last decade, the focus of airlines has shifted from capturing market share to consolidating operations in the most profitable routes. Airlines have also increased the average load factor of flights and have shifted from the under-50 seat regional aircraft towards the 70-90 seat aircraft, which tend to have superior operating economics.[2] This new airline operations paradigm has contributed to the significant loss of connectivity for many regional airports.[3] If an under-50 passenger regional aircraft could be operated economically compared to larger aircraft, then it could potentially encourage airlines to open up new markets, reestablish service at smaller airports, and increase mobility and connectivity for all passengers.

NASA has a vested interest in promoting mobility for the flying public. Much of NASA's aeronautics research portfolio takes guidance and direction from the National Aeronautics Research Plan, which specifically calls out Mobility as a guiding research principal.[4] In addition, NASA's Aeronautics Research Mission Directorate has identified three overarching drivers to guide research planning in its Strategic Implementation Plan (SIP).[5] The first "Mega-Driver" is "Global Growth in Demand for High Speed Mobility." An aircraft that contributes to revitalizing the regional, short-haul segment would both increase mobility and shorten travel times for the flying public. The second "Mega-Driver" is "Global Climate Change, Sustainability, and Energy Use." Although mobility was the driving force behind this study, careful consideration of the environmental impact is still needed for any new aircraft concepts, including the emissions, noise and overall energy usage.

This study targeted a capacity of 48 passengers for a future advanced regional aircraft concept based on market and demand analysis.[6] The year 2030 was selected for introduction of this aircraft concept into the fleet. Based on this entry-into-service year, the design team conducted a technology down-select exercise considering the technologies that could be available in that timeframe. One of the main considerations for the down-select was selecting technologies that might be applied more successfully on a smaller aircraft versus a larger aircraft. Electric propulsion was identified as one such technology. Electric propulsion has historically been applied only to small aircraft due to the experimental nature of the technology. It is reasonable to expect that the first commercial aircraft to use electric propulsion would be a regional or commuter aircraft. Although electric propulsion has advantages in terms of efficiency, major disadvantages include the low specific powers, specific energies, and power densities of current batteries, motors, and power electronics. Even with optimistic projections for these electric systems, an all-electric aircraft introduced in the 2030 time frame is unlikely to have enough range to be competitive with conventional aircraft, even for a regional, short-haul mission. With this in mind, a hybrid-electric propulsion system was proposed as an alternative to an all-electric system. A hybrid-electric system would have many of the advantages of an all-electric propulsion system, yet could take advantage of the superior energy density of jet fuel to overcome some of the disadvantages, such as range. Although a hybrid-electric system would not be able to match the efficiencies of an all-electric propulsion system, it may allow the operating costs of a small regional aircraft to be competitive with much larger aircraft using conventional propulsion systems.

III. Problem Statement

This study focuses on a regional aircraft with a design range of 600 nautical miles carrying 48 passengers. The design range was selected to be consistent with other ongoing NASA hybrid-electric aircraft design studies and is supported by a range sensitivity analysis that examined captured demand versus range for a 48 passenger aircraft.[6] The study mission profile includes takeoff at sea-level, climb to optimum altitude for specific range, cruise at Mach 0.475, descent, and landing. Additional fuel and battery for a reserve mission is also included. The reserve mission consists of 5% reserve fuel as a fraction of total trip fuel, an 87 nautical mile diversion, and a 45 minute continued cruise. This requirement is based on the ATR 42-500 reserve mission requirements for comparison purposes.[7]

The advanced regional aircraft is analyzed with four levels of electrification, 0% electric with 100% conventional, 25% electric with 75% conventional, 50% electric with 50% conventional, and 75% electric with 25% conventional. The results for these different designs are compared to determine the tradeoffs available for a conventional/hybrid-

electric powered regional class aircraft. Each of the four aircraft are designed to minimize the takeoff gross weight (TOGW) on the design mission by varying wing area and maximum takeoff thrust. Design constraints are used to bound the design space and limit the designs to feasible or useful products.

In order to keep the study manageable without missing any significant factors, several assumptions were carefully chosen. The design variables were limited to the wing area and maximum takeoff thrust. Consequently, the fuselage geometry is essentially fixed within each configuration and the tails are resized based on the use of a constant tail volume coefficient. Current technology level is assumed for the baseline aircraft. In other words, the baseline aircraft was calibrated to published data and no additional technology factors or adjustments were made. The advanced aircraft, including the motor, battery, and electric system, are based on technologies projected to be available in the year 2030. This study also assumes a fixed mission for all of the aircraft that is consistent with existing capabilities for a 48 passenger regional transport aircraft. A propulsion system performance deck with a total shaft power of 2400 horsepower is scaled as necessary for each design. This total shaft power is split between the conventional and electric components based on the percent electric desired, impacting the fuel flow and battery discharge rate of the system.

IV. Engine Model Development

Engine models were developed to represent current turboprop engine performance and projected future performance with advanced technology. The basis for the engine modeling was the PW 100 series of engines, which are three shaft, two spool turboprop engines.[8] A representative model of the PW 127E turboprop engine, minus the propeller, was assembled in the NPSS (Numerical Propulsion System Simulation) code for cycle analysis.[9,10,11] NPSS is a component-based, object-oriented engine cycle simulator in which a model is assembled from a collection of interconnected engine components and controlled through the implementation of an appropriate solution algorithm. The PW 127E uses two stages of centrifugal compression providing an overall pressure ratio (OPR) of 14.7. Each compression stage is powered by a single stage turbine, one low pressure and one high pressure. A two stage power turbine provides shaft power to the propeller through a reduction gearbox (2400 shp at static takeoff conditions). The remainder of the fluid momentum provides jet thrust (289 lb at static takeoff conditions). The specific fuel consumption (SFC) is 0.474 lbm/hr/hp at maximum power.[12,13,14,15] The first step of the engine modeling process was to generate an NPSS model that appropriately represents the PW 127E, using component performance measures (e.g., efficiencies) corresponding to the state-of-the-art in components readily available in NPSS to match publicly available data. This model was then exercised throughout the flight envelope. Once an engine model representative of current performance was completed, individual components were then upgraded to predict the overall performance of an advanced version of the engine that could be available in the 2030 time frame.

The NPSS turboprop models were run through the Flight Optimization System's (FLOPS) engine module to add the propellers.[16] FLOPS uses the Hamilton Standard method to estimate the propeller performance. Publically available engine and propeller data was used as input to FLOPS. [12,13,17]

A. Baseline Technology Model

Component efficiencies (η) for the NPSS model of a PW 127E-like engine were estimated using representative values for component performance corresponding to the state of art (SOA) period in the evolution of engine technology.[18] These values are listed in Table 1. The SOA turbine inlet temperature (T4) for a cooled turbine is estimated to be 2860°R and typical compressor bleed flow rates for turbine cooling are assumed. For example, there is 5% bleed from the high pressure compressor to the inlet guide vane (HPC-IGV), 2.5% bleed from the high pressure compressor to the high pressure turbine (HPC-HPT), and 3.5% bleed from the low pressure compressor to the low pressure turbine (LPC-LPT). These estimates combine in the NPSS model to provide the take-off (T/O) performance given in Table 2, which matches the published OPR of 14.7 and SFC of 0.474 lbm/hr/hp at 2400 shp and a jet thrust of 287 lbf. The performance of this engine model was predicted over the flight envelope of altitude (0-30,000 ft), Mach number (0-0.6) and throttle setting (100-10%). Results are presented in Table 2 for static takeoff, rolling takeoff, top of climb, start of cruise, and average cruise.

B. Advanced Technology Model

Component efficiencies (η) for the NPSS model of an advanced turboprop engine were estimated using envisioned values for component performance corresponding to an advanced evolution of engine technology.[18] These values are listed in Table 1. The turbine inlet temperature is left the same as the SOA, but the cooling flow to the inlet guide vanes is zero assuming that they are made of ceramic matrix composites (CMC). The advanced engine model created in NPSS has the same static takeoff OPR, shaft power, and jet thrust as the baseline model as noted in Table 2.

Basically, the advanced engine has 9.8% lower SFC and has 12.3% lower inlet mass flow at sea level static conditions. The performance of this engine model was predicted over the flight envelope of altitude (0-30,000 ft), Mach number (0-0.6) and throttle setting (100-10%). Results are presented in Table 2 for static takeoff, rolling takeoff, top of climb, start of cruise, and average cruise.

Reduced thrust versions of the advanced engine model at 1800 shp (25% electric), 1200 shp (50% electric), and 600 shp (75% electric) were developed for the hybrid-electric propulsion system. These versions have the same OPR and SFC characteristics as the advanced 2400 shp model. This result is dictated by the fact that the PW 100 series engines used as the basis for the cycle modeling are three shaft engines with a separate power turbine shaft driving the propeller gearbox. Since the NPSS models are 1-D and the component efficiencies are assumed the same for the reduced power versions, even though smaller versions would actually see some performance penalty, the output of this power turbine shaft is directly proportional to mass flow. The inlet to exit pressure ratio is also kept the same in the model, setting the exit Mach number to be the same as the 2400 shp model and resulting in a jet thrust proportional to mass flow as well.

Table 1. Current (SOA) and Advanced Engine Component Performance

	SOA	**Advanced**
η Diffuser	0.975	0.975
η LPC	0.86	0.88
η HPC	0.86	0.88
HPC-IGV Cooling (%)	5.0	0
HPC-HPT Cooling (%)	2.5	2.5
LPC-LPT Cooling (%)	3.5	3.5
η Burner	0.95	0.98
Burner Pressure Loss (%)	7.0	7.0
T4 (°R)	2860	2860
η HPT	0.85	0.88
η LPT	0.85	0.88
η PT	0.85	0.88
η Nozzle	0.975	0.985

Table 2. Engine Performance Estimates for SOA and Advanced Engine Technology Levels

	Units	Static T/O	Rolling T/O	Top of Climb	Start of Cruise	Average Cruise
MN		0	0.2	0.5	0.5	0.5
Altitude	ft	0	0	20,000	20,000	20,000
Throttle	%	100	100	100	90	80
SOA						
Power	hp	2,400 (2400*)	2,452	1,696	1,527	1,357
Jet Thrust	lbf	287 (289*)	294	230	206	181
SFC	lbm/hr/hp	0.474 (0.474*)	0.469	0.430	0.432	0.433
Mass Flow	lbm/s	12.15	12.33	7.59	7.32	7.01
OPR		14.7 (14.7*)	14.5	16.8	15.9	14.9
Advanced						
Power	hp	2,400	2,462	1,604	1,443	1,283
Jet Thrust	lbf	287	297	218	194	170
SFC	lbm/hr/hp	0.427	0.423	0.398	0.394	0.391
Mass Flow	lbm/s	10.65	10.85	6.47	6.26	6.01
OPR		14.7	14.6	16.4	15.4	14.4

*Published manufacturer values

C. Engine Flowpath and Weight Estimation

Following the engine cycle model development, estimates of the engine weights and flowpath dimensions were developed. A NASA software tool, WATE++ (Weight Analysis of Turbine Engines), was used to create engine architectures that could achieve the engine thermodynamic cycles produced by the NPSS models detailed in the previous section.[19] The cycle data required for WATE execution, such as air mass flow, temperatures, pressures, pressure ratios, etc., were derived from the NPSS cycle model output. Both the ADP (aerodynamic design point) and off-design cases were used to encompass the maximum performance level (i.e., temperature and pressure) required to size each engine component. The cycle data, the material properties, and design rules for geometric, stress, and turbomachinery stage-loading limits were used to determine an acceptable engine flowpath. For the advanced engines, ceramic-matrix composite HPT inlet guide vanes were assumed, versus nickel-based alloys used for the state-of-the-art engine. An empirical correlation was used to calculate the weight of the gearbox and lubrication system as shown in Figure 1 where hp represents horsepower and RPM represents revolutions per minute. The correlation is a function of maximum delivered output power and gear ratio, and was developed at NASA based on actual gearbox weight data from over fifty rotorcraft, tiltrotor, and turboprop aircraft. [20]

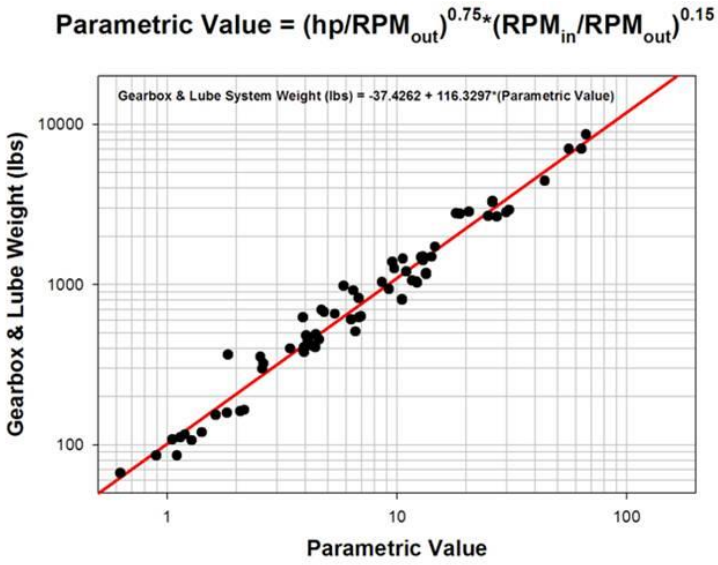

Figure 1. Transmission and lubrication system weight correlation.

For the propeller systems, a rotor weight correlation, which is a function of maximum power delivered to the rotor, propeller tip-speed, and propeller diameter, was used. A weight reduction factor of 20 percent was applied to account for the use of current state-of-the-art materials. The propeller system includes blades, disks, spinner, and pitch-changing mechanism. For the hybrid-electric system, a projected power density of 8 hp/lb was assumed for the motors, and 10 hp/lb for the power electronics. For the current study, it is assumed that the thermal management system is incorporated into the motor casing by using multifunctional structures. [21]

Table 3 gives a summary of the major weights and dimensions of the engines developed for this study. The propeller diameter for all the engines in this study is about 12.8 feet and the nacelle diameter stays constant (about 3.3 feet). For the hybrid-electric engines, it was assumed that the electric motor systems are installed within the engine pods.

Table 3. Principle Turboprop Engine Flowpath Parameters

Mechanical Design Parameter	SOA Turboprop 2400 SHP	Advanced Turboprop 2400 SHP	Advanced Hybrid-Electric Turboprop Gas Turbine + Electric Motor		
			1800 + 600 SHP	1200 + 1200 SHP	600 + 1800 SHP
Turbine engine + Gearbox weight (lb)	1054	1010	819	626	410
Propeller system + Nacelle weight (lb)	782	781	766	752	737
Electrical system weight (lb)	-	-	135	270	405
Total engine weight (lb)	1836	1791	1720	1648	1552
Engine pod length (ft)	7.0	7.0	6.1	5.3	4.2
Maximum Propeller Diameter (ft)	12.8	12.8	12.8	12.8	12.8
Nacelle Diameter (ft)	3.3	3.3	3.3	3.3	3.3

V. Aircraft Model Development

The basis for the aircraft modeling was the ATR 42-500, a twin-turboprop powered, high wing, t-tail configuration. Both baseline technology and advanced technology aircraft models were created in FLOPS.[16] First, the baseline technology model was created and calibrated to known data. Then, technology factors were applied to the baseline model to create the advanced technology aircraft model. ATR 42-500 data was used to calibrate the baseline model.[7,22,23,24] The technology factors for the advanced model were based on previous NASA projects.[25,26] Both aircraft were simulated flying the study mission to enable a direct performance comparison.

A. Baseline Technology Model

An Open Vehicle Sketch Pad (OpenVSP) model was created based on publically available geometry data for the ATR 42-500 (see Figure 2).[27] This model was used to calibrate the wetted area estimates in FLOPS. The initial FLOPS estimate for operating empty weight (OEW) was higher than the published data. Since multiple components of the ATR 42-500 are made of composite materials,[7] adjustments to account for composite construction were made to the FLOPS weight estimates for these component to calibrate the FLOPS OEW to the published data. The FLOPS estimated performance was calibrated using the published payload-range diagram. The engine fuel flow, lift-independent drag, and lift-dependent drag factors were used as calibration parameters. No source was found for the cruise altitudes and velocities used to generate the published payload-range diagram; therefore, they were also allowed to vary during the calibration. The calibration process resulted in the baseline aircraft shown in Table 4. The results of simulating both the ATR 42-500 baseline calibration mission (840nm) and the baseline study mission (600nm) is shown in Table 4.

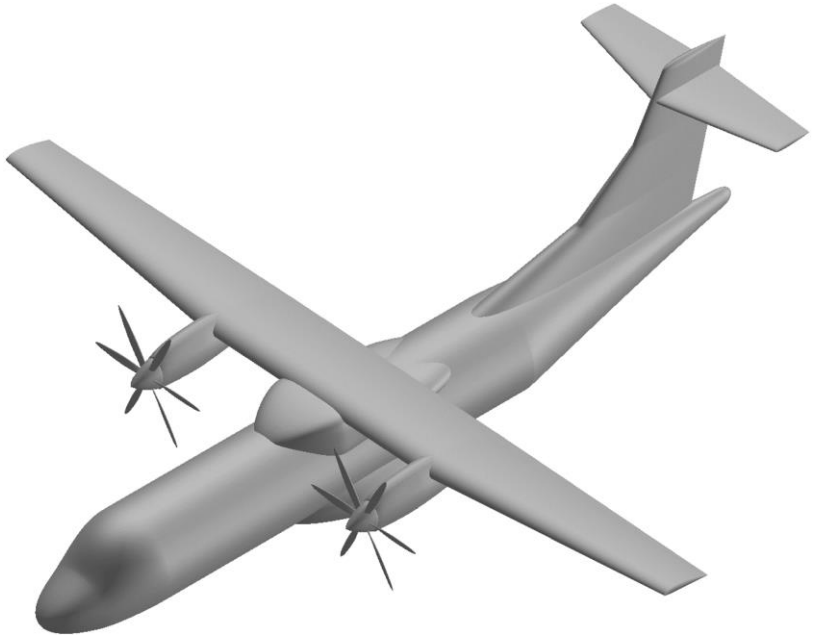

Figure 2. OpenVSP model of the baseline aircraft

B. Advanced Technology Model

Technology factors were added to the baseline technology aircraft model to create the advanced model. The following technologies were used on the advanced aircraft:

1) Damage Arresting Stitched Composites
2) Advanced Sandwich Composites
3) Metal Matrix Composites and Ceramic Matrix Composites (landing gear)
4) Hybrid-Electric Aircraft Architecture
5) Lightweight Electrical Systems
6) Lightweight Cabin Furnishings
7) Natural Laminar Flow (wing, horizontal tail, vertical tail)

The aircraft weight reduction technologies were applied as reduction factors. The electric aircraft architectures were assumed to replace most or all of the hydraulic systems; however, a conservative estimate of no weight reduction was used due to lack of weight data on the electrical systems replacing the hydraulics. Similarly, for the "Lightweight

Electrical Systems" technology the electrical systems were assumed to be lighter, but increased in quantity resulting in no electrical system weight savings. A weight reduction in cabin furnishings was estimated using information from an ATR marketing brochure.[28] NASA Ames Research Center 12 ft. wind tunnel test data were used to estimate the extent of natural laminar flow on the wing and tail surfaces.[29] The performance of the advanced aircraft flying the study mission (600nm) is shown in Table 4.

Table 4. Baseline and Advanced Aircraft Characteristics and Mission Performance

	Units	**Baseline**	**Baseline**	**Advanced**
Design Mission		Calibration	Study	Study
Mission Parameters				
TOGW	lb	41,000	40,700	35,900
OEW	lb	24,800	24,800	21,800
Payload	lb	10,100	10,800	10,800
Number of Passengers		48	48	48
Design Range	nm	840	600	600
Total Mission Fuel	lb	6,200	5,100	3,300
Block Fuel	lb	4,600	3,700	2,200
Aircraft Parameters				
Wing Area	ft^2	590	590	510
Wing Span	ft	81	81	76
AR		11	11	11
Wing Loading, W/S	lb/ft^2	70	70	70
Cruise Velocity	kts	295	300	300
Start of Cruise L/D		13	11	15
Start of Cruise CL		0.377	0.307	0.502
Start of Cruise CD		0.0290	0.0272	0.0326
Start of Cruise Altitude	ft	18,800	9,500	24,900
Thrust per Engine	lb	8,400	8,400	7,300
Start of Cruise TSFC	lb/hr/lb	0.507	0.526	0.423

VI. Multi-Disciplinary Optimization Framework

A new analysis framework was created specifically for this study. A low-order multi-disciplinary optimization (MDO) environment was created that could capture the unique features of parallel hybrid-electric aircraft. The Flight Optimization System (FLOPS) is utilized to develop aerodynamic, weight, propulsion, geometry, and performance data for the vehicles.[16] ModelCenter is used as a platform to connect FLOPS with engine deck files created within Excel as well as battery energy and weight calculations.[30] The current MDO framework does not capture the detailed coupling and interactions among different disciplines such as aerodynamics and structures to save computing time. For this effort, there was a focus on low computing time to enable analysis in minutes rather than hours or weeks.

A. Hybrid-Electric Aircraft Sizing Procedure

The use of two sources of energy introduces additional complications in aircraft sizing. Aircraft sizing typically involves determining the takeoff weight, wing area, and engine thrust required to perform the design mission while meeting necessary performance requirements such as minimum rate-of-climb and maximum approach speed. For a conventional aircraft, the fuel weight required to complete the mission drives the aircraft sizing. For a hybrid-electric aircraft, the energy storage system (e.g., battery) becomes an additional weight that is also a function of the mission and aircraft characteristics. The FLOPS aircraft synthesis code includes a basic capability for analysis of electric and hybrid-electric aircraft. However, hybrid-electric *propulsion*, such as the parallel hybrid system considered here, cannot be directly analyzed in FLOPS. FLOPS allows two different propulsion systems with different types of energy sources to be defined, resulting in a hybrid aircraft. But, only one propulsion system can be operating during any given segment of the mission. In other words, it is not possible to have both a battery and fuel providing propulsive energy at the same time as is the case in a parallel hybrid propulsion system. Because of this limitation, the electric propulsion capabilities of FLOPS were not used in this study. Instead, FLOPS was used as a mission analysis core with external analyses providing the necessary inputs to perform the complete aircraft sizing.

Figure 3 shows the overall process flow for the aircraft sizing procedure. Necessary inputs include: gas turbine performance (shaft power, nozzle thrust, and fuel flow vs. Mach, altitude, and throttle setting) and weight data; propeller performance (thrust vs. power, Mach, altitude) and weight data; overall electric system efficiency (from energy storage to shaft power) and weight data; energy storage specific energy; level of electrification; and a FLOPS model of the basic non-hybrid aircraft. Three key simplifying assumptions are made for the analysis in this study. First, the level of electrification (% of shaft power provided by the electric system) is constant throughout the mission. In other words, "50% electric" means that the electric motor is providing 50% of the total shaft power at all times. This limitation is inherent in the approach used. Given this simplifying assumption, it is not possible to use this process to size vehicles with a more varied concept of operations, such as using electric power only in certain phases of the flight or optimizing the power split at different points in the mission. The second key simplification is that the gas turbine performance (i.e., specific fuel consumption) is independent of its rated output. In reality, it is expected that as more of the power is provided by the electric system and the size of the gas turbine decreases, the gas turbine performance will degrade. Appropriate performance scaling laws were not available for the class of turbine engines used in the study and therefore specific fuel consumption was held constant with size. The sizing procedure in Figure 3 does not, however, preclude the inclusion of such degradation in the methodology. The final key simplification is that the efficiency of the electric power system is invariant with the power output. In reality, the efficiencies of the electric system components will be a function of the electrical load.

The gas turbine performance input in Figure 3 is for the all-turbine, zero electric power case. For a given level of electrification, this information is used to create a new propulsion performance deck for input to FLOPS. In generating the hybrid engine deck, the shaft power is held the same as the all-turbine case at all conditions independent of level of electrification, as the electric motor plus gas turbine is assumed to generate the same total shaft power as the all-turbine case. The level of electrification does impact the fuel flow and nozzle thrust at each condition, however. For example, for a 25% electric, the original fuel flow and nozzle thrust values are multiplied by 0.75 since the gas turbine is sized to only provide 75% of the power. (The fuel flow factor could be adjusted further to account for gas turbine scaling effects as discussed above.) Although fuel flow is reduced by the addition of electric power, the electric power obviously does not come for free and it is necessary to track the amount of electric energy being used in order to size the electric energy storage appropriately. Fortunately, there is another input in the FLOPS engine deck besides fuel flow that is integrated over the course of the mission analysis. Typically this input is used to track NO_X emissions during the mission. However, in this case the electric system "energy flow" for each condition, that is, power output of the electric energy storage system, is placed in the NO_X input field. The energy storage system power output is calculated from the electric shaft power output at each condition and the user provided overall electric efficiency. For example, consider a case in which the total shaft power output of the propulsion system is 1000 kW, the electrification is 25%, and the overall electric efficiency is 90%. The energy storage system power output would be 0.25*1000/0.9 = 278 kW. Stated another way, the rate of energy use from the storage system would be 278 kWh per hour. The hybrid propulsion system performance is provided to FLOPS as a "thrust deck" (thrust, fuel flow, and energy flow vs. M, altitude, and throttle) by using the propeller performance data to determine propeller thrust and adding the gas turbine nozzle thrust. Reference 31 provides more details on the process for creating a thrust deck using shaft power and nozzle thrust data. In the MDO framework, the hybrid engine deck is generated in a spreadsheet and provided to the FLOPS analysis.

When the energy flow from the hybrid propulsion thrust deck is integrated over the entire mission by FLOPS, the result is the total electric energy used during the primary mission. Unfortunately, since FLOPS does not integrate the NO_X emissions input field for the reserve mission segments, the method used to calculate the total energy for the primary mission cannot be used for the reserve segments. Reserve energy requirements are instead estimated from the correlation between mission and reserve fuel for the conventional (0% electric) case. Another consideration for electric energy storage is the maximum depth-of-discharge. In the case of batteries, for example, there is a limit to how much of the stored energy can be used without damaging the battery. It was assumed for the current study that 80% of the energy storage system capacity could be discharged routinely without damage based on current state-of-the-art lithium-ion batteries.[32] The energy storage system is sized, therefore, such that the primary mission energy and a majority of the reserve mission energy is within this 80% constraint. However, to avoid oversizing the re-useable portion of the energy storage for rare, emergency situations (for example, a flight at the maximum design range which also expends all of its fuel/energy reserves), a portion of the reserve mission energy is allocated beyond the 80% depth-of-discharge constraint. The storage system would have to be replaced after a flight which used this emergency reserve energy. The required mission and reserve energy combined with the constraint on depth-of-discharge results in a required energy storage capacity in kWh. The user provided electric storage specific energy combined with the required capacity provides an estimate of the energy storage weight. In the FLOPS analysis this weight is simply input as cargo. (This assumes the energy storage system has a fixed weight throughout the mission. Storage systems that

increase or decrease in weight as they are discharged cannot be modeled with this approach.) As shown in Figure 3, FLOPS is executed in an iterative loop until the storage weight assumed is equal to the storage weight required. During each of the iterations, FLOPS is internally performing an iteration on the required fuel load to meet the mission requirements. In other words, for a given energy storage weight input, FLOPS is sizing the takeoff and fuel weights and providing an output of the electric energy use, which is then used to update the storage system weight estimate. Once converged, the weight allocated for electric energy storage on-board the aircraft is consistent with the electric energy requirements for the mission.

The Design Explorer optimization tool in ModelCenter is used to size the wing area and propulsion system to meet a series of performance constraints. As the required thrust/power of the propulsion system changes during the optimization, the FLOPS internal propulsion system scaling is used. Since FLOPS has been provided a hybrid engine deck and hybrid propulsion system weight, this means that the entire propulsion system is scaled together and the level of electrification (split in total shaft power between turbine and electric motor) remains constant during the sizing.

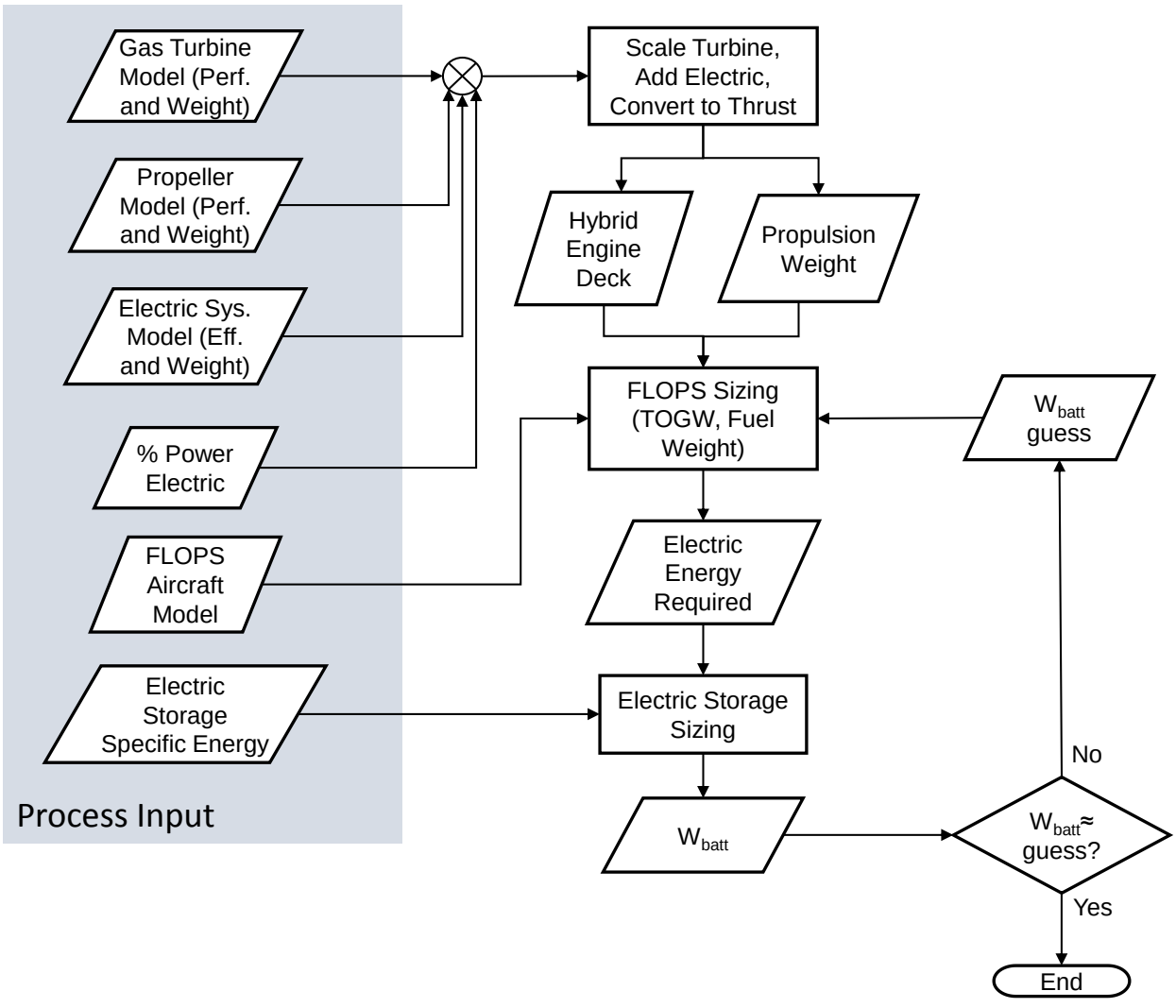

Figure 3. Hybrid-electric aircraft sizing process intergrated into ModelCenter.

B. Design Objectives

The design objectives drive the multi-disciplinary design and optimization (MDO). Given enough freedom in constraints and design variables, completely different aircraft can result from a MDO with a different design objective. The design objective chosen for the study was minimum Takeoff Gross Weight (TOGW).

C. Design Variables

The design variables used in this study are limited to the wing area and maximum takeoff thrust. Variation in these two parameters is necessary to meet performance constraints such as maximum approach speed and takeoff field length as the TOGW of the designs vary.

D. Design Constraints

The design constraints bound the problem. They are used in this study to ensure adequate aircraft performance. The design constraints are as follows:

1) Range: The range of the aircraft must be greater than or equal to 600 nm with enough fuel and battery capacity to complete the reserve mission.
2) Approach Speed: The approach speed must not exceed 140 knots.
3) Takeoff Field Length: The takeoff field length must not exceed 7,000 feet.
4) Landing Field Length: The landing field length must not exceed 7,000 feet.
5) Missed Approach: The missed approach thrust margin with one engine inoperative must be greater than zero.
6) Second Segment Climb: The excess thrust available during the second segment climb with one engine inoperative must be greater than zero.
7) Excess Fuel Capacity: The wing must have enough fuel volume to carry the required mission fuel plus reserves. The excess fuel capacity must be greater than zero.
8) Instantaneous Rate of Climb for Climb Ceiling: The instantaneous rate of climb for the climb ceiling must be greater than or equal to 300 ft/s.
9) Reserve Segment: The aircraft must carry an additional 5% reserve fuel as a fraction of total trip fuel and be capable of flying an 87 nautical mile range diversion, and a 45 minute cruise segment after the design mission missed approach. This requirement is based on the ATR 42-500 reserve mission requirements for comparison purposes.[7]

VII. Results

Both level of electrification and battery specific energy were varied to observe their effect on the aircraft system. Twelve different aircraft designs were created and analyzed encompassing 0, 25, 50, and 75 percent electric with battery specific energy values of 500, 750, and 1000 Wh/kg. Full tabular results including the variation in aircraft weights, fuel consumption, energy consumption, and energy cost are provided in the Appendix.

Figure 4 displays the effect of battery specific energy and percent electric on the battery, fuel, and total energy consumption of the system. A few observations can be made:

- The battery energy and fuel energy are equal at ~66% electric. Recall that the percent electric is based on shaft power, not energy used.
- As the level of electrification increases, total energy used by the system increases for a BSE of 500 Wh/kg. However, for 750 and 1000 Wh/kg, the total energy decreases. This decrease in total energy occurs because of the higher efficiency of the electric propulsion even though the weight of the aircraft is increasing.

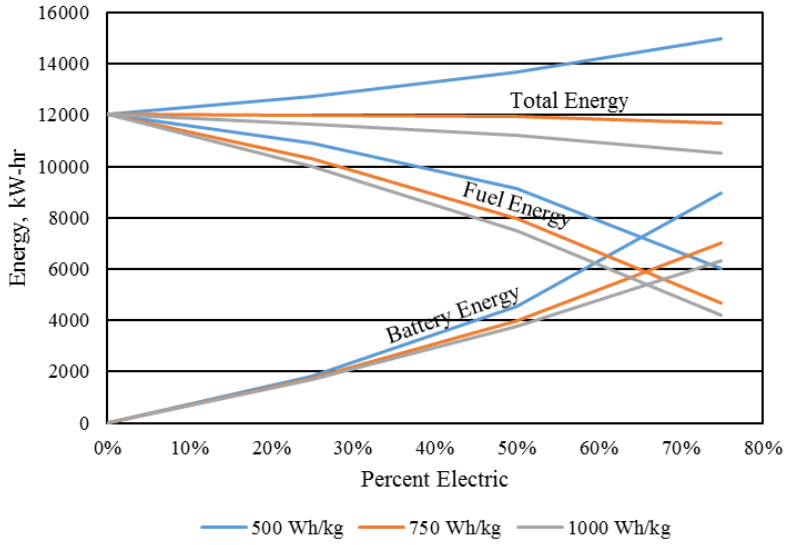

Figure 4. Battery energy, fuel energy, and total energy.

Figure 5 displays the effect of battery specific energy and level of electrification on the takeoff gross weight (TOGW) and operating empty weight (OEW). Historically, the total life-cycle costs of an aircraft have had a strong correlation to the takeoff gross weight and the acquisition cost to the operating empty weight. A few observations can be made:

- Assuming a BSE of 500 Wh/kg, a 75% hybrid-electric aircraft would be 2.3 times heavier than a 0% electric advanced turboprop.
- Assuming a BSE of 750 Wh/kg, a 75% hybrid-electric aircraft would be 63 percent heavier than a 0% electric advanced turboprop.
- Assuming a BSE of 1000 Wh/kg, a 75% hybrid-electric aircraft would be 39 percent heavier than a 0% electric advanced turboprop.
- The operating empty weight of the aircraft was not significantly influenced by the increase in electrification. The higher takeoff gross weights are primarily a result of the weight of the energy storage system.

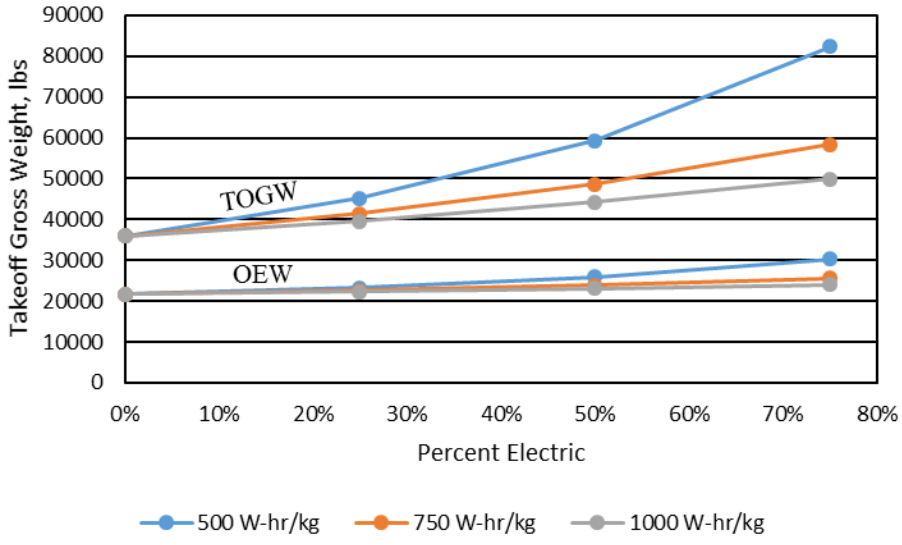

Figure 5. Takeoff and operating empty weight.

Figure 6 displays the effect of battery specific energy and level of electrification on the total energy cost in the year 2030. The projections for the price of Jet-A fuel and electricity were calculated as an average of multiple projections for 2030 from the U.S. Energy Information Administration.[33] These average prices were $3.33 per gallon for Jet-A fuel and $0.11 per kWh for electricity. The Jet-A price was converted to $0.09 per kWh using a conversion factor of 36.3 kWh/gallon. A few observations can be made from the following results:

- Assuming a BSE of 500 Wh/kg, energy costs for a 75% electric hybrid aircraft would be 42 percent more than for a 0% electric advanced turboprop.
- Assuming a BSE of 750 Wh/kg, energy costs for a 75% electric hybrid aircraft would be 11 percent more than for a 0% electric advanced turboprop.
- Assuming a BSE of 1000 Wh/kg, energy costs for a 75% electric would be 0.4 percent less than for a 0% electric advanced turboprop.

These energy cost results are highly dependent on the prices assumed for electricity and jet fuel. There are other forecast scenarios which result in the relative energy costs of the hybrid electric aircraft being more or less favorable.

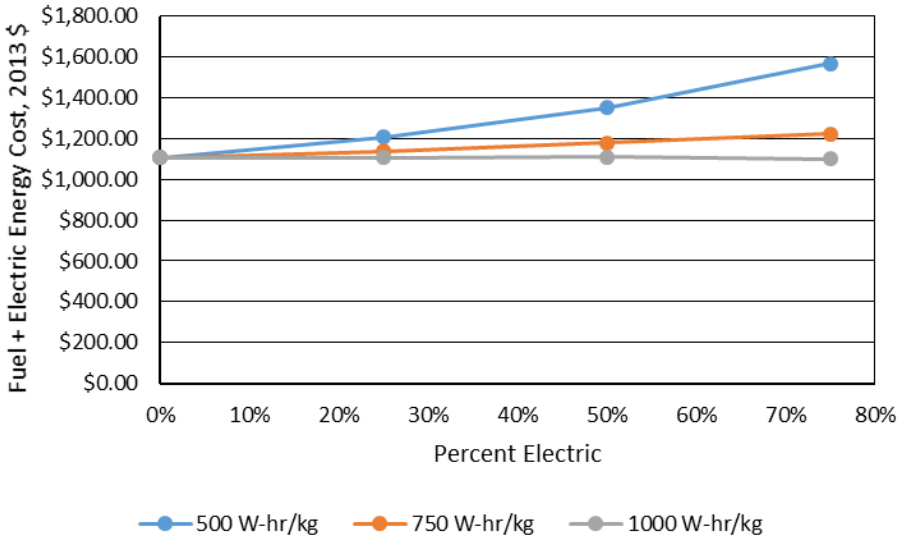

Figure 6. Total (fuel + electric) energy cost based on projections for 2030.

VIII. Conclusions

This study focuses on a regional aircraft with a design range of 600 nautical miles carrying 48 passengers. The aircraft is analyzed with four levels of electrification: 0% electric with 100% conventional, 25% electric with 75% conventional, 50% electric with 50% conventional, and 75% electric with 25% conventional. The aircraft is also analyzed with three values for battery specific energy, 500, 750, and 1000 Wh/kg.

The conclusions drawn from this study are presented below. At the size and range of the advanced turboprop:

1. The battery specific energy must be 750 Wh/kg or greater for the total energy to be less than for a conventional aircraft.
2. A hybrid vehicle would likely not be economically feasible with a battery specific energy of 500 or 750 Wh/kg based on the higher gross weight, operating empty weight, and energy costs compared to a conventional turboprop.
3. The battery specific energy would need to reach 1000 Wh/kg by 2030 to make the electrification of its propulsion an economically feasible option for the reasons outlined in the previous conclusion.

Note that the weight and energy trades for electrification are likely to be more favorable with a shorter range design mission, for which the difference in the energy density of electric strorage and jet fuel represents less of a penalty. The hybrid-electric aircraft also has potential benefits not considered in this study, such as the potential for a reduced carbon footprint when the energy storage system is charged from renewable sources. Another benefit is the potential for more synergistic propulsion-airframe integration than with conventional propulsion. In the current study no changes were made to the propulsion-airframe integration to take advantage of the additional flexibilities offered by electric propulsion. Alternative concepts exploiting these flexibilities should be examined.

Appendix

A. Tabular Output for a Battery Specific Energy of 500 Wh/kg

	Units	0% Electric	25% Electric	50% Electric	75% Electric
Operating Empty Weight	lb	21,749.1	23,289.8	25,855.4	30,294.3
Payload Weight	lb	10,800	10,800	10,800	10,800
Total Fuel Weight	lb	3,339.6	3,100.1	2,596.0	1,719.6
(Block Fuel Weight)	*lb*	*2,223.0*	*2,013.9*	*1,682.5*	*1,108.7*
Battery Weight	lb	0	8,036.6	20,097.9	39,585.5
Takeoff Gross Weight	lb	35,922.5	45,226.5	59,349.4	82,399.4
Wing Area	ft^2	498.8	590.2	786.3	1,168.0
Thrust per Engine	SLS, lb	7,332.0	8,832.0	11,085.9	14,718.8
Max Electric Power per Engine	kW	0	472.61	1,186.47	2,362.78
Fuel Energy	kWh	12,049.63	10,916.21	9,119.88	6,009.64
Battery Energy	kWh	0	1,822.25	4,557.21	8,982.19
Total Energy	kWh	12,049.63	12,738.46	13,677.09	14,991.83
Electric Energy Cost	$	$0.00	$205.91	$514.96	$1,014.99
Fuel Energy Cost	$	$1,104.86	$1,000.94	$836.23	$551.04
Total Energy Cost	$	$1,104.86	$1,206.85	$1,351.19	$1,566.03

B. Tabular Output for a Battery Specific Energy of 750 Wh/kg

	Units	0% Electric	25% Electric	50% Electric	75% Electric
Operating Empty Weight	lb	21,749.1	22,622.3	23,854.4	25,612.5
Payload Weight	lb	10,800	10,800	10,800	10,800
Total Fuel Weight	lb	3,339.6	2,910.7	2,258.4	1,334.8
(Block Fuel Weight)	*lb*	*2,223.0*	*1,897.6*	*1,467.2*	*864.3*
Battery Weight	lb	0	5,051.4	11,708.8	20,637.5
Takeoff Gross Weight	lb	35,922.5	41,384.5	48,621.6	58,384.9
Wing Area	ft^2	498.8	544.9	623.4	775.5
Thrust per Engine	SLS, lb	7,332.0	8,320.3	9,652.3	11,390.6
Max Electric Power per Engine	kW	0	445.23	1,033.00	1,828.56
Fuel Energy	kWh	12,049.63	10,285.82	7,952.86	4,684.88
Battery Energy	kWh	0	1,717.93	3,981.95	7,025.16
Total Energy	kWh	12,049.63	12,003.75	11,934.81	11,710.04
Electric Energy Cost	$	$0.00	$194.13	$449.96	$793.84
Fuel Energy Cost	$	$1,104.86	$943.14	$729.22	$429.57
Total Energy Cost	$	$1,104.86	$1,137.26	$1,179.18	$1,223.41

C. Tabular Output for a Battery Specific Energy of 1000 Wh/kg

	Units	0% Electric	25% Electric	50% Electric	75% Electric
Operating Empty Weight	lb	21,749.1	22,318.2	23,040.6	24,040.9
Payload Weight	lb	10,800	10,800	10,800	10,800
Total Fuel Weight	lb	3,339.6	2,820.0	2,121.1	1,197.6
Block Fuel Weight	*lb*	*2,223.0*	*1,844.2*	*1,379.3*	*776.7*
Battery Weight	lb	0	3,684.4	8,264.2	13,940.2
Takeoff Gross Weight	lb	35,922.5	39,622.6	44,225.8	49,978.7
Wing Area	ft^2	498.8	523.8	555.1	645.3
Thrust per Engine	SLS, lb	7,332.0	8,089.8	9,066.4	10,226.6
Max Electric Power per Engine	kW	0.00	432.88	970.28	1,641.72
Fuel Energy	kWh	12,049.63	9,996.37	7,476.41	4,210.05
Battery Energy	kWh	0.00	1,670.16	3,746.93	6,323.22
Total Energy	kWh	12,049.63	11,666.53	11,223.34	10,533.27
Electric Energy Cost	$	$0.00	$188.73	$423.40	$714.52
Fuel Energy Cost	$	$1,104.86	$916.59	$685.53	$386.03
Total Energy Cost	$	$1,104.86	$1,105.32	$1,108.94	$1,100.56

Acknowledgments

Thank you to those who contributed and members of the Short Haul team: William Fredericks, Andrea Storch, Jason Welstead (NASA Langley Research Center), and William Haller (NASA Glenn Research Center). This study was supported by NASA's Advanced Air Transport Technology project.

References

[1]Shankland, S., "Airbus shows E-Fan, its electric plane due in 2017", *CBS Interactive Inc.*, URL: http://www.cnet.com/news/airbus-shows-e-fan-its-electric-plane-due-in-2017/

[2]Bachman, J., "Think Planes Are Crowded? There's Room for Things to Get Worse.," *Bloomberg Business*, 06 September 2013.

[3]Wittman, M.D., and Swelbar, W.S., "Trends and Market Forces Shaping Small Community Air Service in the United States," May 2013. URL: http://dspace.mit.edu/bitstream/handle/1721.1/78844/Trends%20and%20Market%20Forces%20Small%20Community.pdf.

[4]National Science and Technology Council, "National Aeronautics Research and Development Plan," February 2010. URL: https://www.whitehouse.gov/sites/default/files/microsites/ostp/aero-rdplan-2010.pdf.

[5]National Aeronautics and Space Administration, "National Aeronautics Research Mission Directorate Strategic Implementation Plan," Washington D.C., 2015.

[6]Marien, T., "Seat Capacity Selection for an Advanced Short-Haul Aircraft Design", *AIAA Modeling and Simulation Technologies Conference*, San Diego, CA, 4-8 January 2016, (submitted for publication)

[7]ATR, "ATR 42-500 A New Standard of Excellence," *Alenia Aeronautica and EADS Brochure*, 2007.

[8]Pratt & Whitney Canada, "PW 100 | PW 150," URL: http://www.pwc.ca/en/engines/PW100%20%7C%20PW150. [Accessed 26 October 2015].

[9]Lytle, J., "The Numerical Propulsion System Simulation: An Overview," NASA TM-2000-209915, 2000.

[10]NPSS Consortium, "NPSS User Guide Software Release: 2.3.0," The Ohio Aerospace Institute, Cleveland, 2010.

[11]NPSS Consortium, and NASA Glenn, "NPSS Reference Sheets Software Release: NPSS 1.6.5," NASA, Cleveland, 2008.

[12]Federal Aviation Administration, "Type Certificate Data Sheet E20NE, Revision 12," U.S. Deparment of Transportation, Washington D.C., 2008.

[13]European Safety Agency, "Type Certificate Data Sheet, Number IM E041, Ussue 02," European Aviation Safety Agency, Koln, 2008.

[14]Bushnell, S., Willis, D., and Jackson, P., "IHS Jane's Aero-Engines, No. 28," IHS Global Limited, Colorado, 2010.

[15]Aviation Week and Space Technology, Aerospace Source Book, Vol. 148, No. 2, 1998.
[16]McCullers, L.A., "Aircraft Configuration Optimization Including Optimized Flight Profiles. Multidisciplinary Analysis and Optimization Part 1," NASA CP-2327, 1984.
[17]Federal Aviation Administration, "Type Certificate Data Sheet P8BO," U.S. Department of Transportation, 2007.
[18]Mattingly, J., Elements of Gas Turbine Propulsion, McGraw-Hill, Inc., 1996.
[19]Tong, M., and Naylor, B., "An Object-Oriented Computer Code for Aircraft Engine Weight Estimation," NASA TM-2009-215656, 2009.
[20]Baum, J.A., Dumais, P.J., Mayo, M.G., Metzger, F.B., Shenkman, A.M., and Walker, G.G., "Prop-Fan Data Support Study Technical Report," NASA CR-152141, 1978.
[21]Dever, T., et. al., "Assessment of Technologies Noncryogenic Hybrid Electric Propulsion," NASA TP-2015-216588, 2015.
[22]ATR, "ATR 42-500 Unrivalled Performance," *ATR DC/E Marketing Brochure*, September 2014.
[23]Federal Aviation Administration, "Type Certificate Data Sheet A53EU," U.S. Department of Transportation, 2014.
[24]Bushnell, S., Willis, D., and Jackson, P., "IHS Jane's All the World's Aircraft 2013-2014: Development and Production 104th Edition. pp. 359-361," IHS Global Limited, Colorado, 2013.
[25]Aerospace Systems Design Laboratory, "FY2013 Environmentally Responisible Aviation Systems Analysis Report: Technology Portfolio and Advanced Configurations," Atlanta, 2013.
[26]Bradley, M., and Droney, C., "Subsonic Ultra Green Aircraft Research: Phase 1 Final Report," NASA CR-2011-216847, 2011.
[27]Hahn, A., "Vehicle Sketch Pad: A Parametric Geometry Modeler for Conceptual Aircraft Design," 48th AIAA Aerospace Sciences Meeting and Exhibit, Orlando, FL, January 2010.
[28]ATR, "ATR-600 Series: The New Armonia Cabin," *ATR DC/E Marketing Brochure*, 2012.
[29]Wagner, R., Maddalon, D., Bartlett, D., Collier, J.F., and Braslow, A., "Laminar Flow Flight Experiments," in *Transonic Symposium: Theory, Application, and Experiment*. *NASA-CP-3020*, Hampton, 1988.
[30]"PHX ModelCenter Desktop Trade Studies," *Phoenix Integration, Inc. Website*, [online database], URL: http://www.phoenix-int.com/software/phx-modelcenter.php, [cited 25 Nov. 2013].
[31]Antcliff, K.R., "Investigation of the Impact of Turboprop Propulsion on Fuel Efficiency and Economic Feasibility," Virginia Tech, Blacksburg, 2014.
[32]Panasonic, "Lithium Ion: NCR18650B," Version 13.11 R1, SANYO Energy Corporation, 2012. URL: http://na.industrial.panasonic.com/sites/default/pidsa/files/ncr18650b.pdf
[33]U.S. Energy Information Administration, "Annual Energy Outlook 2015 with Projections to 2040," U.S. Department of Energy, April 2015, URL: http://www.eia.gov/forecasts/aeo/pdf/0383(2015).pdf